Toxicology and Applied Pharmacology 322 (2017) 15–26

Contents lists available at ScienceDirect

Toxicology and Applied Pharmacology

journal homepage: www.elsevier.com/locate/taap

Embryotoxic and pharmacologic potency ranking of six azoles in the rat whole embryo culture by morphological and transcriptomic analysis

Myrto Dimopoulou [a,b,*], Aart Verhoef [b], Jeroen L.A. Pennings [b], Bennard van Ravenzwaay [a,d], Ivonne M.C.M. Rietjens [a], Aldert H. Piersma [b,c]

[a] Division of Toxicology, Wageningen University, The Netherlands
[b] National Institute of Public Health and the Environment (RIVM), Bilthoven, The Netherlands
[c] Institute for Risk Assessment Sciences, Utrecht University, Utrecht, The Netherlands
[d] BASF SE, Experimental Toxicology and Ecology, Ludwigshafen, Germany

ARTICLE INFO

Article history:
Received 15 December 2016
Revised 9 February 2017
Accepted 1 March 2017
Available online 3 March 2017

Keywords:
Whole embryo culture
Toxicogenomics
Azoles
Retinoic acid
Embryonic development
Sterol biosynthesis

ABSTRACT

Differential gene expression analysis in the rat whole embryo culture (WEC) assay provides mechanistic insight into the embryotoxicity of test compounds. In our study, we hypothesized that comparative analysis of the transcriptomes of rat embryos exposed to six azoles (flusilazole, triadimefon, ketoconazole, miconazole, difenoconazole and prothioconazole) could lead to a better mechanism-based understanding of their embryotoxicity and pharmacological action. For evaluating embryotoxicity, we applied the total morphological scoring system (TMS) in embryos exposed for 48 h. The compounds tested showed embryotoxicity in a dose-response fashion. Functional analysis of differential gene expression after 4 h exposure at the ID_{10} (effective dose for 10% decreased TMS), revealed the sterol biosynthesis pathway and embryonic development genes, dominated by genes in the retinoic acid (RA) pathway, albeit in a differential way. Flusilazole, ketoconazole and triadimefon were the most potent compounds affecting the RA pathway, while in terms of regulation of sterol function, difenoconazole and ketoconazole showed the most pronounced effects. Dose-dependent analysis of the effects of flusilazole revealed that the RA pathway related genes were already differentially expressed at low dose levels while the sterol pathway showed strong regulation at higher embryotoxic doses, suggesting that this pathway is less predictive for the observed embryotoxicity. A similar analysis at the 24-hour time point indicated an additional time-dependent difference in the aforementioned pathways regulated by flusilazole. In summary, the rat WEC assay in combination with transcriptomics could add a mechanistic insight into the embryotoxic potency ranking and pharmacological mode of action of the tested compounds.

1. Introduction

Supranational regulatory guidelines, such as the European legislation of Registration, Evaluation, Authorization and Restriction of Chemicals (REACH), demand the use of large numbers of experimental animals for the risk assessment of chemicals (Scialli and Guikema, 2012). Reproductive and developmental toxicity studies require almost 65% of experimental animals needed overall (Scialli and Guikema, 2012; van der Jagt et al., 2004). The necessity of reduction, refinement and replacement of animal testing has stimulated the design and application of alternative assays for the hazard identification of developmental toxicants (Augustine-Rauch et al., 2010; Piersma, 2006; Scialli, 2008). Alternative techniques vary from cell-based methods to organ culture, organ-on-a-chip, whole embryo cultures to *in silico* simulation models (Piersma, 2006; Lee et al., 2012; Spielmann, 2009).

The rat whole embryo culture (WEC) technique is an alternative method for assessing possible developmental toxicants, and it is used for screening studies due to its numerous benefits (Genschow et al., 2002; Piersma, 2004). This technique allows the continuous monitoring of embryonic development during gestational days (GD) 10 to 12, when a major part of organogenesis occurs (New et al., 1976). Additionally, the complexity of the entire embryo is included, and development mimics the *in vivo* situation in terms of both morphology and gene expression signatures (Robinson et al., 2012a). The limitations of this method include the restricted experimental duration and the absence of metabolic activity, as well as the lack of maternal interaction. Various metabolic systems added to WEC have shown activity (Piersma, 1993; Webster et al., 1997). However, even with the addition of metabolic activity, some classes of proembryotoxicants would not be classified properly in *in vitro* testing systems, such as the WEC (Luijten et al., 2008). Furthermore, it has been suggested that direct testing of the parent

* Corresponding author at: Wageningen University, Division of Toxicology, P.O. Box 8000, 6708WE Wageningen, The Netherlands.
E-mail address: myrto.dimopoulou@wur.nl (M. Dimopoulou).

http://dx.doi.org/10.1016/j.taap.2017.03.001
0041-008X/

compounds and metabolites individually might provide a solution if metabolic pathways are known (Webster et al., 1997; Luijten et al., 2008; Flick et al., 2009). Overall, the rat WEC is considered a valuable tool for screening xenobiotics and prioritizing further steps in risk assessment of possible embryotoxicants (Ellis-Hutchings and Carney, 2010; Piersma et al., 1995; Sogorb et al., 2014). Previous studies have shown that apart from screening morphological endpoints for evaluating possible developmental toxicants in the WEC model, the implementation of technologically advanced molecular-based assays could improve its value as a predictive assay (Piersma, 2006; Robinson et al., 2012b; Robinson et al., 2016). Previous studies have shown that gene expression changes, related to toxic responses of biological systems, are not only associated with morphological outcomes, but also precede them (Balmer et al., 2014). Additionally, literature data indicate that different compounds might cause a similar adverse outcome, while the underlying mechanisms of toxicity might be different. Transcriptomics approaches could enhance mechanistic knowledge of embryotoxicants (Robinson et al., 2016; Daston and Naciff, 2010). An additional advantage of transcriptomics is that the evaluation of molecular signatures could contribute to the identification of biomarkers for detecting embryotoxicity among different classes of compounds (Robinson et al., 2016; Hermsen et al., 2011). Furthermore, due to the high conservation of many molecular pathways, these biomarkers could improve the extrapolation of results obtained from *in vitro* studies to the *in vivo* situation and contribute to understanding interspecies differences (Daston and Naciff, 2010; Robinson et al., 2012c).

Azoles form a class of compounds, known for their potential to induce teratogenic effects in mammals in a dose dependent manner (de Jong et al., 2011; Menegola et al., 2006a). They are fungicides with either agricultural or clinical use. Their mode of pharmacological action in the fungal cell is based on the inhibition of the conversion of lanosterol to ergosterol *via* disturbing the enzyme involved being *Cyp51*, which is the mediator for securing the robustness of fungal membranes (Marotta and Tiboni, 2010; Zarn et al., 2003). The toxicological mechanism of azoles is partly unknown. However, when *in vivo* and *in vitro* mammalian systems are exposed to either azoles or retinoic acid (RA), a variety of similar teratogenic responses have been observed, including abnormalities in craniofacial development, brain segmentation and branchial arches formation (Cunningham and Duester, 2015; McCaffery et al., 2003; Li et al., 2012; Luijten et al., 2010). Therefore, azoles might have a shared mechanism of toxicological action with RA-induced embryotoxicity, which is supported by gene expression studies showing that the enzyme *Cyp26a1*, a key regulator of embryonic RA concentration, was upregulated in a common manner (Luijten et al., 2010; Dimopoulou et al., 2016; Menegola et al., 2006b). Thus, *Cyp26a1* and *Cyp51* appear as candidate biomarkers for embryotoxicity and pharmacologic activity of azoles, respectively. However, this does not exclude that other mechanisms may be involved as well.

In order to assess the usefulness of transcriptomics readouts in assessing relative embryotoxic potencies and the underlying modes of action, we have studied the morphologic and transcriptomic responses of six azoles in WEC and compared their potencies with existing *in vivo* data. We included flusilazole (FLU) (Farag and Ibrahim, 2007; Lamontia et al., 1984), triadimefon (TDF) (Machemer, 1976; Unger et al., 1982) and ketoconazole (KTZ) (Nishikawa et al., 1984; Tachibana et al., 1987) as relatively strong embryotoxicants *in vivo*; miconazole (MCZ) (Ito et al., 1976) as weak embryotoxicant; difenoconazole (DFZ) (Lochry, 1987) and prothioconazole (PTZ) (Stahl, 1997) as non-embryotoxicants.

2. Materials and methods

2.1. Animal care

Animal studies were approved and performed in concordance with institutional and federal regulations at the National Institute of Public Health and the Environment (RIVM). Wistar rats (HsdCpd:WU) (Harlan, The Netherlands) were housed at the RIVM Animal Care facility in a climate-controlled room with a 12 h light cycle (04:00–16:00 dark). Water and food were provided *ad libitum*. After acclimating for 2 weeks, virgin female rats were housed with male rats for a 3-hour mating period (9:00–12:00) (GD 0). Mated dams were individually housed. The clinical condition of all the animals was monitored daily.

2.2. Rat whole embryo culture

The WEC technique was performed in accordance with the validated method of Piersma (2004). On GD 10, between 9:00 and 12:00 a.m., dams were euthanized by intracardiac injection of T61^R (Intervet, The Netherlands). Rat embryos were immediately separated from the uterus. The peripheral trophoblastic cell zone and parietal yolk sac membrane were removed under the microscope leaving both the visceral yolk sac and ectoplacental cone intact. Embryos with 1–5 somites were cultured for morphological assessment while embryos with 2–4 somites were cultured for gene expression studies, which increases precision of the embryonic stage sufficient for gene expression analysis (Luijten et al., 2010). Embryos were separately cultured in flasks with 2 mL culture medium, which was a mixture of 90% pregnant bovine serum and 10% rat serum (Biochrom, Berlin, Germany), diluted with 14% Hank's solution (Gibco) and supplemented with 1.6 mg/mL D-glucose and 75 μg/mL L-methionine (Sigma-Aldrich, Zwijndrecht, The Netherlands). Afterwards, the culture flasks were placed in rotating incubators, which were completely protected from light and their internal temperature was permanently at 37.7 °C. The cultured flasks were oxygenated twice daily for 30 s per time, with increasing concentration of oxygen: on the first day (GD10) at 9:00 and 16:00 (5% O_2, 5% CO_2, 90% N_2), on the second day (GD11) at 9:00 and 16:00 (20% O_2, 5% CO_2, 75% N_2) and on the third day (GD12) at 9:00 (40% O_2, 5% CO_2, 55% N_2).

2.3. Morphological assessment and statistical analysis of individual endpoints

Embryos (exposed to test compounds and controls) were cultured for 48 h (whole culture period; 0–48 h) and were scored according to the TMS system taking into account 20 morphological endpoints (Brown and Fabro, 1981). These morphological endpoints were subdivided into groups, which included growth parameters (yolk sac diameter, crown-rump length, head diameter and number of somites) and developmental/functional parameters, such as yolk sac and allantoic blood circulation, heart formation and heart beating, embryo- turning, caudal neural tube, optic and otic system, fore- and hind- limb, branchial arches, mandibular and maxillary process and the shape and size of somites. Average scores of each of the morphological endpoints were calculated for identifying any possible specific and selective embryotoxic effects of the tested compounds in rat embryos.

Within each exposure group, including also the vehicle control (DMSO), 8 rat embryos were evaluated. For normalizing the obtained data and eliminating daily variation, the embryos within the same exposure group were derived from different dams and they were cultured over different culture days. Statistical analysis was performed using the parametric Student's *t*-test (unpaired), two-sided, and with 95% confidence intervals. Images of the examined embryos (exposed for 48 h to either DMSO or tested compounds) were obtained using an Olympus SZX9 camera and Olympus DP software. The pictures were taken at ×20 magnification. For specific observations, ×32 magnification was used.

2.4. Test compounds and exposure concentrations

The following six azoles were tested in rat WEC for 48 h (0–48 h) in a range of concentrations with the lowest concentration inducing no

morphological effect to the highest being the maximal achievable concentration in culture:

Difenoconazole (DFZ; CAS# 119446-68-3, Sigma-Aldrich, Zwijndrecht, The Netherlands) at 20, 60, 200 and 600 μM; flusilazole (FLU; CAS# 85509-19-9, Sigma-Aldrich, Zwijndrecht, The Netherlands) at 2, 6, 20, 60, 200 and 600 μM; ketoconazole (KTZ; CAS# 65277-42-1, Sigma-Aldrich, Zwijndrecht) at 2, 6, 20, 60 and 200 μM; miconazole (MCZ; CAS# 22916-47-8, Sigma-Aldrich, Zwijndrecht, The Netherlands) at 2, 6, 20, 60, 200 and 600 μM; prothioconazole (PTZ; CAS# 178928-70-6, Sigma-Aldrich, Zwijndrecht, The Netherlands) at 60, 200 and 600 μM and triadimefon (TDF; CAS# 43121-43-3, Sigma-Aldrich, Zwijndrecht, The Netherlands) at 20, 60, 200 and 600 μM. All the compounds were dissolved in dimethyl sulfoxide (DMSO, Sigma-Aldrich, Zwijndrecht, The Netherlands), and all embryos were exposed to a final DMSO concentration of 0.1%. As it has been previously described, this concentration of DMSO did not significantly alter the morphology (4, 24 and 48 h) and has limited effects on gene expression after either 4 h or 24 h of exposure at the same concentration (0.1%) (Robinson et al., 2012a; Robinson et al., 2012c; Robinson et al., 2010). For finding the appropriate concentration at which the microarrays were conducted, we calculated the concentration which results to 10% reduction of the control TMS (ID_{10}) with both PROAST (Slob, 2002) and Graphpad software (www.graphpad.com). Therefore, for microarray analysis, rat WEC were exposed for 4 h (0–4 h) to FLU at testing concentrations of 0.002, 0.02, 0.2, 2, 25, 200 μM (tenfold concentration intervals) for 4 h (0–4 h), while they were also exposed to the established ID_{10} of 25 μM for 24 h (0–24 h). The remaining compounds were tested in the rat WEC for 4 h (0–4 h) at their ID_{10} values: DFZ at 110 μM, KTZ at 40 μM, MCZ at 25 μM and TDF at 150 μM, as derived from the concentration response curves on TMS. Rat embryos which were treated with PTZ were exposed to the calculated ID_{10} (250 μM) and at 60 μM. All the treated embryos were immediately collected after the end of their exposure and stored for performing the microarray analysis.

2.5. Whole embryo RNA isolation

For transcriptomics, cultured embryos were quickly scored on the basis of their somite number, their position in the yolk sac, neural tube developmental stage, crown-rump length and head diameter. They were then isolated from the yolk sac and ectoplacental cone, placed in 200 μM RNAlater (Ambion, Austin, Texas), stored for one week at 4 °C, and then stored for further processing at −80 °C with the lowest possible amount of RNAlater. After the embryos were thawed on ice, they were separately homogenized by passing them 10 times though a 1 mL syringe with a 26G needle. The RNA of the homogenized lysate was further isolated by using the RNeasy Micro Plus RNA isolation kit (CAS number 74034, Qiagen, the Netherlands). Eluting with 14 μM of RNase-free H_2O, final volumes of 12 μL RNA were obtained and tested on both Nanodrop (Nanodrop Technologies Inc., Wilmington, Delaware) and 2100 BioAnalyzer (Agilent Technologies, Palo Alto, California) to establish the RNA quality and quantity. The RNA samples with an absorbance value between 1.9 and 2.2 (ratio 260 mm/280 mm) and RNA integrity number (RIN) higher than 7,

Table 1
Representative pictures of rat WEC exposed to the tested azoles at a range of concentrations for 48 h. The morphology of embryos exposed at the lowest concentration of each compound was identical with those in the control group (DMSO).

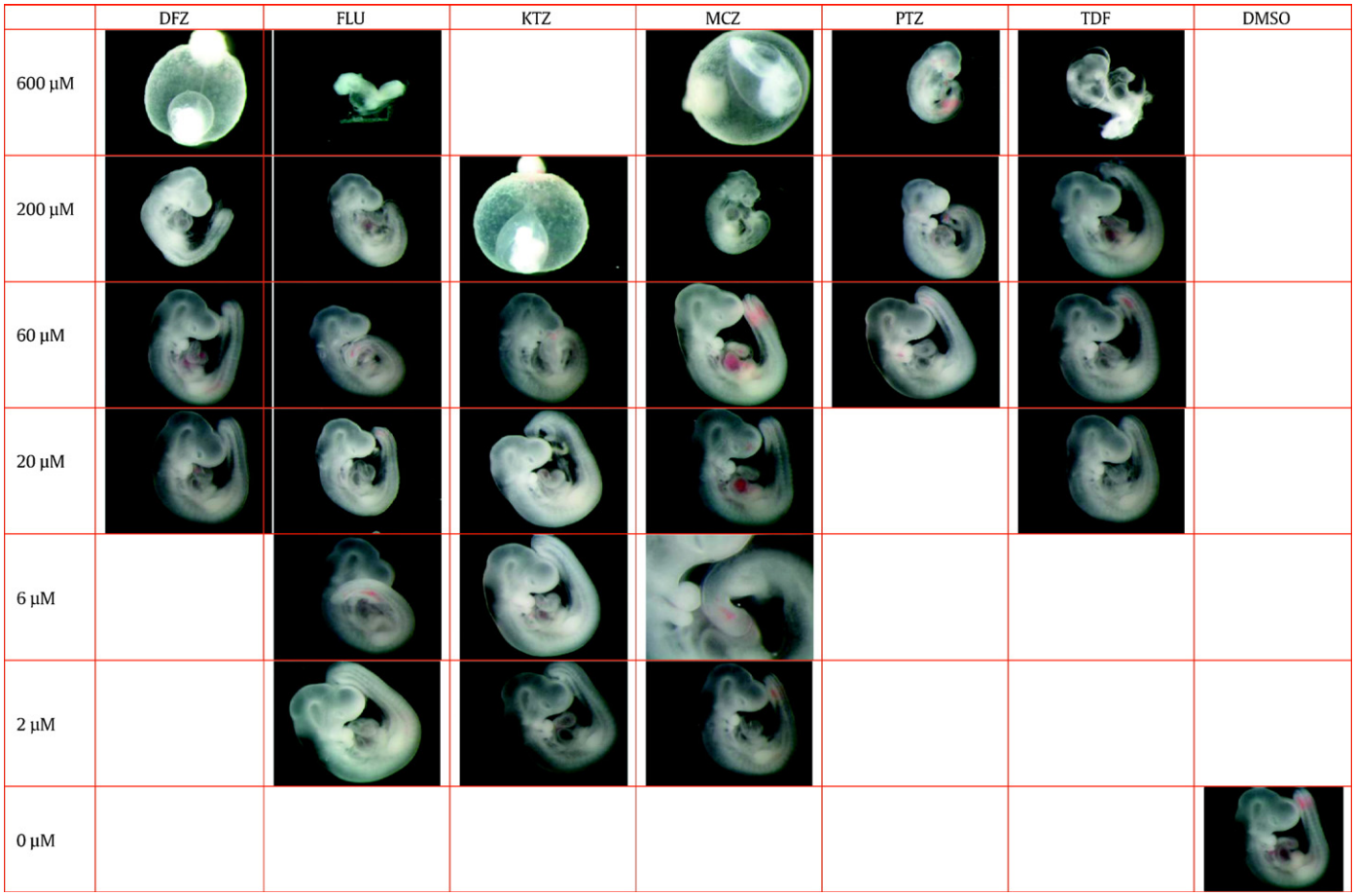

The pictures were taken at ×20 magnification. For specific observations, ×32 magnification was used.

were further used for performing the microarray analysis. RNA samples were stored at −80 °C.

2.6. Microarray hybridization

RNA hybridization and microarray experimentation were performed by the Dutch Service and Support Provider (MAD) of the University of Amsterdam, the Netherlands. In brief, for every sample, RNA was amplified, biotin-labelled and hybridized to Affymetrix GeneChip HT RG-230 PM Array Plates according to the provided protocols by Affymetrix (Santa Clara, CA). After staining, the HT Array plate was read by the Affymetrix GeneChip® HT Scanner and analysed by the Affymetrix GeneChip® Operating Software. For performing the aforementioned steps, the GeneTitan® Hybridization, Wash, and Stain Kit for 3′ IVT Arrays (cat no. 901530) was used. In total, 112 arrays were analysed. For the exposure to compounds tested at singe concentrations, 8 embryos per compound were prepared, while for the exposure to FLU for which more than one concentration was tested, 7 embryos for each concentration were included.

2.7. Microarray analysis and data processing

The quality control (QC) and the normalization of the microarray data were performed using the ArrayAnalysis.org webpage (www.arrayanalysis.org) (Eijssen et al., 2013), designed by the Department of Bioinformatics in Maastricht University. Raw microarray values were inspected for their quality by assessing the 3′/5′ ratios for β-actin and GAPDH, RNA degradation, background intensity, signal quality and the probe-set homogeneity with NUSE (Normalized Unscaled Standard Error) and RLE (Relative Log Expression). After the QC, two samples were excluded from the analysis because they did not fulfil the aforementioned quality criteria. The Affymetrix CEL files were further normalized by using the Robust Multichip Average (RMA) algorithm (Irizarry et al., 2003) and the Brainarray custom CDF version 19 probe set annotation (http://brainarray.mbni.med.umich.edu/Brainarray/default.asp) (Dai et al., 2005). In total, 13,877 probe sets, each corresponding to an Entrez Gene ID, were further evaluated by performing a statistical analysis in R (www.R-project.org) and Microsoft Excel.

2.8. Identification of differentially expressed genes

Normalized data was transformed to log scale. For each exposure group (*i.e.* a compound at a concentration and time point), gene expression data were compared to the appropriate control (unexposed embryos at the same time point), for calculating absolute average fold changes of individual gene expression. Differentially expressed genes were identified by using ANOVA, using a p-value < 0.001 and a False Discovery Rate (FDR) of 10%, as stringency criteria. Genes differentially expressed in at least one of the 8 or 7 rat WEC samples from the corresponding exposure groups were combined for further analysis.

Gene expression responses were visualized using a heatmap combined with hierarchical clustering (Euclidean distance, Ward linkage) as well as Principal Component Analysis (PCA). Each bar in the heatmap represents the average of the gene expression in the experimental group compared to the appropriate control group.

2.9. Functional interpretation analysis of differentially expressed genes

Functional annotation and overrepresentation analysis were performed using DAVID (https://david.ncifcrf.gov/) (Huang da et al., 2009). Additionally, functional annotations were added from the literature (Robinson et al., 2012d; Tonk et al., 2015). For genes involved in RA pathway, general development and sterol biosynthesis pathway, gene

Table 2
Overview of morphological effects of the tested azoles in the rat WEC assay.

Compound	Concentration (μM)	TMS	CRL (mm)	$S_{48\ h} - S_{0\ h}$	FORE	MID	HIND	CAUD	OTIC	OPTIC	BRAN	MAND-MAX	SOM	HEART
DMSO	0	67.4 ± 0.8	4.2 ± 0.2	24 ± 1.1	–	–	–	–	–	–	–	–	–	–
DFZ	20	66.1 ± 2.1	4.1 ± 0.2	24 ± 0.5	–	–	–	–	–	–	–	–	–	–
	60	65.4 ± 1.4	4.1 ± 0.2	23 ± 1.4	–	–	–	*	–	–	–	–	–	–
	200	50.2 ± 2.2**	3.1 ± 0.2****	18 ± 1.6*	*	**	**	**	**	*	*	**	*	*
	600	14.8 ± 0.9****	#	#	***	**	***	***	****	***	***	****	***	***
FLU	2	66.6 ± 0.5	4.2 ± 0.2	24 ± 1.2	–	–	–	–	–	–	–	–	–	–
	6	66.0 ± 1	4.2 ± 0.2	24 ± 0.3	–	–	–	–	–	–	–	–	–	–
	20	60.8 ± 4.7	4.0 ± 0.3	22 ± 1.6	–	–	–	–	–	–	–	–	–	–
	60	53.9 ± 2.6*	3.9 ± 0.2	17 ± 2.0	–	–	–	*	–	–	–	–	–	–
	200	37.4 ± 9.1***	3.2 ± 0.2****	15 ± 3.0*	*	**	**	**	***	*	*	**	–	*
	600	18.6 ± 2.5****	1.5 ± 0.5****	9 ± 0.7**	***	**	***	****	****	**	**	****	**	***
KTZ	2	66.9 ± 1.2	4.2 ± 0.2	23 ± 0.7	–	–	–	–	–	–	–	–	–	–
	6	66.8 ± 1.2	4.2 ± 0.2	24 ± 0.5	–	–	–	–	–	–	–	–	–	–
	20	63.3 ± 2.5	4.1 ± 0.3	23 ± 1.7	–	–	–	–	–	–	–	–	–	–
	60	54.4 ± 3.7*	3.9 ± 0.3	16 ± 1.8	–	–	–	*	–	–	–	–	–	–
	200	15.6 ± 0.5***	#	#	*	**	**	**	***	*	*	*	**	*
MCZ	2	66.7 ± 0.8	4.1 ± 0.2	24 ± 0.5	–	–	–	–	–	–	–	–	–	–
	6	63.0 ± 7.6	4.1 ± 0.3	23 ± 2.5	–	–	–	–	–	–	–	–	–	–
	20	61.0 ± 3.4	4.0 ± 0.2	22 ± 1.5	–	–	–	–	–	–	–	–	–	–
	60	58.3 ± 6.2*	4.1 ± 0.3	23 ± 1.2	–	–	–	*	–	–	–	–	–	–
	200	30.2 ± 6.1***	2.9 ± 0.7****	13 ± 2.7*	*	**	**	**	***	*	*	**	–	*
	600	20.6 ± 3.6****	#	12 ± 2.1**	***	***	***	****	****	**	**	****	**	***
PTZ	60	65.8 ± 4.2	4.1 ± 0.3	24 ± 1.1	–	–	–	–	–	–	–	–	–	–
	200	62.4 ± 2.6**	3.9 ± 0.2	23 ± 1.1	*	*	*	*	**	*	*	*	**	–
	600	33.1 ± 9.8****	2.7 ± 0.4****	10 ± 2.7**	***	***	***	***	***	***	**	***	***	***
TDF	20	66.4 ± 1.1	4.1 ± 0.2	24 ± 0.8	–	–	–	–	–	–	–	–	–	–
	60	65.4 ± 1.1	4.1 ± 0.2	24 ± 0.9	–	–	–	*	–	–	–	–	–	–
	200	55.8 ± 5.1**	3.8 ± 0.2**	20 ± 2.2*	*	**	**	**	**	*	*	**	*	*
	600	18.8 ± 2.4****	2.4 ± 0.2****	10 ± 3.4***	***	***	***	***	****	***	***	****	***	***

Each number represents a mean ± SD (N = 8, Student's *t*-test: * p < 0.05, ** p < 0.005, *** p < 0.0005, **** p < 0.0001). CRL: crown-rump length; S_{48h} - S_{0h}: number of somites that formed during the culture period of rat WEC; FORE: forebrain; MID: midbrain; HIND: hindbrain; CAUD: caudal neural tube; OTIC: otic system; OPTIC: optic system; BRAN: branchial arches; MAND-MAX: mandibular and maxillary process; SOM: quality of somites and HEART: heart; "#": could not be measured.

expression data per pathway were combined to absolute average fold changes per pathway. Next, the absolute average fold changes per exposure group were plotted against the compound concentration used. In the case of FLU multiple concentrations were tested, allowing data for other compounds to be compared against the flusilazole dose-response curve to assess the relative potency in each pathway.

Finally, gene expression and functionality were visualized as a network using Cytoscape version 2.8.3 (www.cytoscape.org) (Smoot et al., 2011).

2.10. In vivo data analysis

A literature survey was performed to determine the *in vivo* developmental toxic profile of the six tested azoles. We selected studies performed in rats orally exposed to the tested compounds during either GD6-15 or GD7-16 at multiple dose regimes. Studies with at least one control group and two dose groups were selected to allow analysis using the Benchmark Dose (BMD) approach. The BMD values were calculated on the basis of an increase in the incidence of skeletal malformations or cleft palate, selected as sensitive endpoints of *in vivo* developmental toxicity. A concentration-response curve was fitted to the data to determine the BMD for the selected benchmark response (BMR) for each tested azole. The BMD was defined as 10% additional incidence of skeletal malformations or cleft palate (BMD_{10}). The BMD_{10} of each compound was calculated with the PROAST software (Slob, 2002) using dichotomous concentration-response models (quantal data). Several models were fitted, included gamma, logistic, loglogistic, probit, logprobit, multistage and Weibull. The selection of the best model was determined based on the goodness of fit (p-value > 0.05), given also the lowest BMD value.The developmental lowest effect levels (dLEL), obtained from the EPA ToxREF database (USEPA, 2016), were also considered for comparison.

3. Results

3.1. Morphological assessment and definition of ID_{10} values

All azoles induced developmental toxicity in a dose dependent manner in the WEC assay (Tables 1 & 2). Highest concentrations without statistically significant effects on TMS were 20 μM for FLU, KTZ and MCZ, and 60 μM for DFZ, PTZ and TDF, respectively. At embryotoxic concentrations, FLU, KTZ and MCZ mostly affected the closure of the neural tube, the formation of branchial arches and early organogenesis of the optic cup. PTZ and DFZ were less potent but showed comparable abnormalities such as somitogenesis and disturbance of closure of the neural tube, as well as retarded development of both otic and optic cups at high doses. On the other hand, TDF affected the development of the branchial arches and the neural tube, while not affecting any of the other morphological endpoints. After evaluating the TMS concentration-response curves in the rat WEC, the ranking of decreasing potency of the six tested azoles was KTZ, MCZ, FLU, DFZ, TDF and PTZ (Fig. 1). The ID_{10} concentrations of all tested compounds were calculated from Fig. 1 to apply them as exposure concentrations in subsequent WEC experiments for performing transcriptomic analysis.

3.2. Microarrays and identification of significant responses

Rat embryos were exposed to ID_{10} concentrations of azoles detected in the WEC assay based on the TMS score to study effects on the level of their transcriptome. Embryos exposed to ID_{10} concentrations for either 4 or 24 h had not yet developed any morphologically observable alterations. For example, somitogenesis, a general hallmark of the progress of embryo development, was unaffected (Fig. 2, A and B).

Gene expression data were analysed by comparing each compound with the control group using ANOVA with significance threshold $p \leq 0.001$ (*t*-test) and an FDR value of 10%. Fig. 3 shows an overview

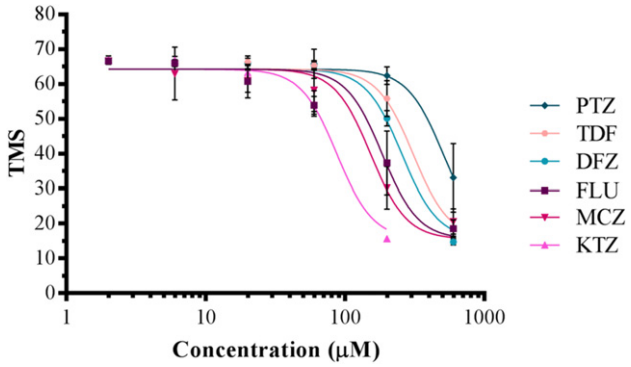

Fig. 1. Total Morphological Score (TMS) concentration responses of 6 azoles in rat WEC after 48 h of culture. Each point represents a mean ± SD (N = 8).

of gene expression changes of the 87 genes showing statistically significant responses. Using DAVID for functional annotation of significantly regulated genes, three main enriched gene groups were identified: RA pathway, general development and sterol biosynthesis pathway. The numbers of genes that were included in these pathways was 12, 29 and 17, respectively (Table 3). The genes in the RA pathway were a subset of the list referred to as the general development related genes.

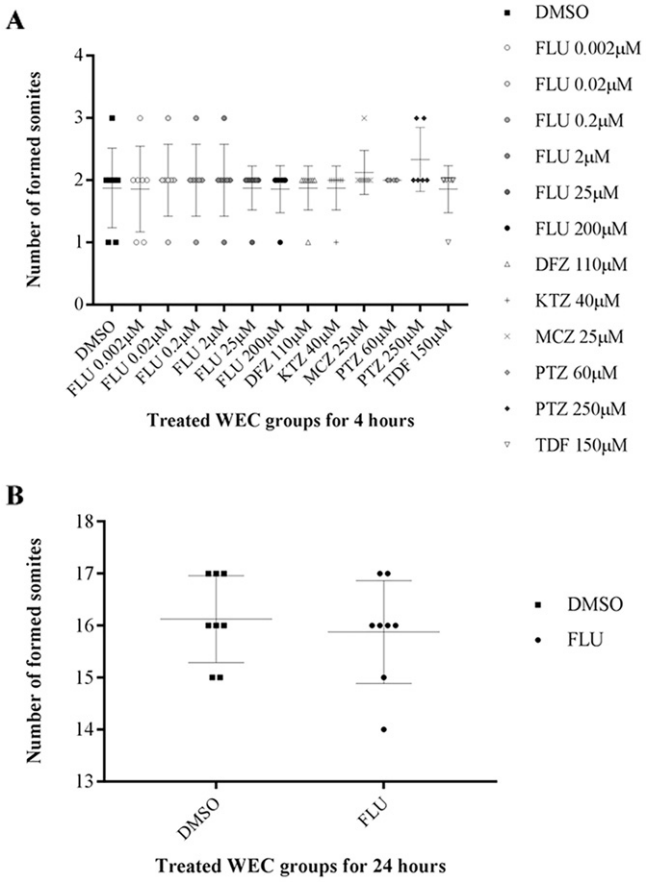

Fig. 2. Somitogenesis in rat embryos exposed to the six tested azoles for 4 h (A) or 24 h (B) and further used for microarray analysis. Each point represents the mean ± SD of embryos which belong in the same group of exposure. The number of embryos per group is N = 8 for single doses per treatment (for 4-hour treatments: DMSO, FLU 25 μM, DFZ 110 μM, KTZ 40 μM, MCZ 25 μM, TDF 150 μM, and for 24-hour treatments: DMSO, FLU 25 μM). The number of embryos exposed for 4 h to FLU is N = 7 for each dose (0.002, 0.02, 0.2, 2, 200 μM).

3.3. Network analysis: relating exposures to pathways and responsive genes

Fig. 4 illustrates the relationships between exposures, genes and pathways as observed in the present study (Fig. 3) using Cytoscape network visualization. Generally, this network analysis demonstrates that embryonic 4-hour exposure to FLU and TDF at or, for FLU, above the ID_{10} provoked an up- or down-regulation of genes involved in general embryonic development and in the RA pathway. In contrast, embryonic exposure to KTZ or DFZ at their respective ID_{10}, for 4 h was primarily linked to the dysregulation of genes related to the sterol biosynthesis pathway. Prolonged exposure of rat embryos at 25 μM of FLU caused a notable upregulation of genes related to the sterol biosynthesis pathway, while the response of the genes participating in the general embryonic development and the RA pathway was varied from up- to down-regulation. PTZ and MCZ were the two compounds with the least effects on the embryonic pathways and the involved genes under investigation.

3.4. Concentration-dependence of gene expression changes

Fig. 5 illustrates the absolute average fold change of the expression of genes participating in the three aforementioned biological pathways upon exposure to increasing concentrations of FLU. Clearly, the lowest FLU concentration tested already showed regulation of each of the three pathways considered. All pathways responded concentration dependently on exposure to FLU. The RA pathway showed the highest magnitude of regulation. The sterol biosynthesis pathway regulation was substantially affected at the highest concentration tested (200 μM), whereas the general development pathway already showed a response at lower concentrations. At the ID_{10} of FLU (25 μM), the RA pathway and general embryonic development showed a more pronounced effect compared to the sterol biosynthesis pathway, at given fold change of 1.41, 1.27 and 1.07, respectively.

Within pathways, individual genes showed differences in responses. In the general development gene set, *Tbx4* was upregulated in a concentration-dependent manner, while *Hoxa1* was downregulated with the same trend (Fig. 3). However, the expression of both genes was almost not altered when rat embryos were exposed at 25 μM (ID_{10}). As to the RA pathway and general development, in 4 h-

Table 3
Gene-set compositions of the three main enriched gene groups: RA pathway, general development and sterol biosynthesis pathway. The numbers of genes included in these pathways is 12, 29 and 17, respectively.

RA pathway (12)	General development (29)	Sterol biosynthesis pathway (17)
Hoxa1	*Hoxa1*	*Pcsk9*
Gbx2	*Gbx2*	*Srebf2*
Fgf4	*Fgf4*	*Sc5d*
Cyp26a1	*Cyp26a1*	*Msmo1*
Hoxc4	*Hoxc4*	*Scd1*
Rarb	*Rarb*	*Cyp51*
Fgfr4	*Fgfr4*	*Hmgcr*
Cyp26b1	*Cyp26b1*	*Sqle*
Dhrs3	*Dhrs3*	*Hsd17b7*
Hoxc10	*Hoxc10*	*Fdft1*
Mafb	*Mafb*	*Hmgcs1*
Wnt5a	*Wnt5a*	*Nsdhl*
	Jund	*Pmvk*
	Ngfr	*Abca1*
	Alx1	*Dhcr7*
	Dlx5	*Mvd*
	Lhx1	*Idi1*
	Sostdc1	
	Mecom	
	Ifrd1	
	Btg2	
	Pcsk9	
	Srebf2	
	Glis2	
	Tbx4	
	Nrip1	
	Cbln1	
	Fgfbp3	
	Tgm2	

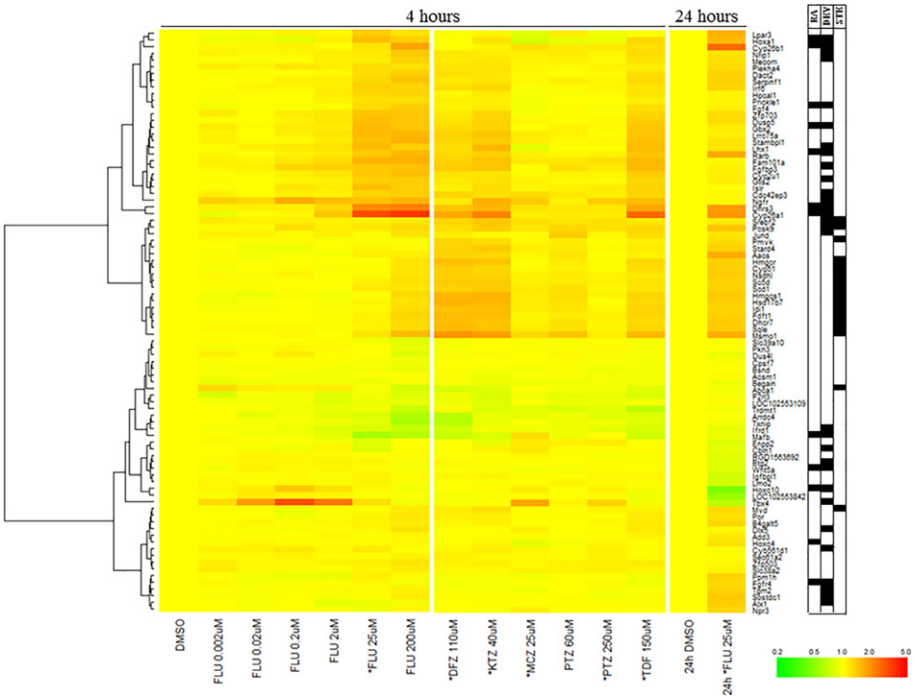

Fig. 3. Hierarchical clustering of gene expression in rat embryos exposed to six azoles. In total 87 genes were significantly regulated after at least one of the treatments. Each bar in the heatmap represents the average of the gene expression in the experimental group compared to the appropriate control group. The 87 genes were further categorized into three groups of biological processes RA pathway (RA), general embryonic development (DEV) and sterol biosynthesis pathway (STE), illustrated as black bars on the right part of this figure.

exposed embryos at 25 μM of FLU there was a pronounced up regulation of *Cyp26a1*, *Dhrs3*, *Gbx2*, *Lhx1*, *Hoxa1* and *Wnt5a*. Their expression was quantified to be respectively 3.0, 2.0, 1.5, 1.5, 1.5 and 1.2 fold higher compared to the control. *Tbx4* and *Mafb* were expressed in a more pronounced way at concentrations lower than the ID_{10}. Sterol-related genes were expressed with slight fluctuations and revealed a remarkable 1.2 fold upward trend when embryos were exposed to 200 μM. Some of the genes in this pathway that did not follow this general trend were *Abca1*, which showed an upward trend at the lowest dose of 0.002 μM of FLU, while *Pcsk9* and *Msmo1* had an upward trend of expression at 25 and 200 μM. Some other representative genes which contributed to the enrichment of the sterol biosynthesis pathway, such as *Cyp51*, *Sqle*, and *Hmgcr*, did show a regular rise of their absolute fold change in response, up to 1.3 fold at the highest concentration of FLU tested.

3.5. Comparing gene set responses at the morphological ID_{10} of six azoles

The potency of the six tested azoles as to the regulation the three functional gene groups was assessed at the ID_{10} of each compound individually. FLU dose-response curves (Fig. 5) were used for comparison.

FLU exposure at its ID_{10} showed a greater response on the RA pathway (1.41) compared to the five remaining ID_{10} exposures. The other compounds, in the order of TDF > KTZ > DFZ > MCZ > PTZ, showed a decreasing magnitude of response on the RA pathway at their ID_{10} (Fig. 6, A), quantified to 1.33, 1.24, 1.17, 1.13 and 1.08 fold, respectively. The commonly most responsive genes were *Cyp26a1*, *Dhrs3* and *Gbx2*. On the other hand, *Wnt5a* was the least responsive and *Mafb* was the most downregulated with the exception of a slightly but not statistically significant upregulated response to MCZ (1.23 fold change) (Fig. 3). Exposure to FLU (1.3) and TDF (1.25) at their ID_{10} resulted in a similar

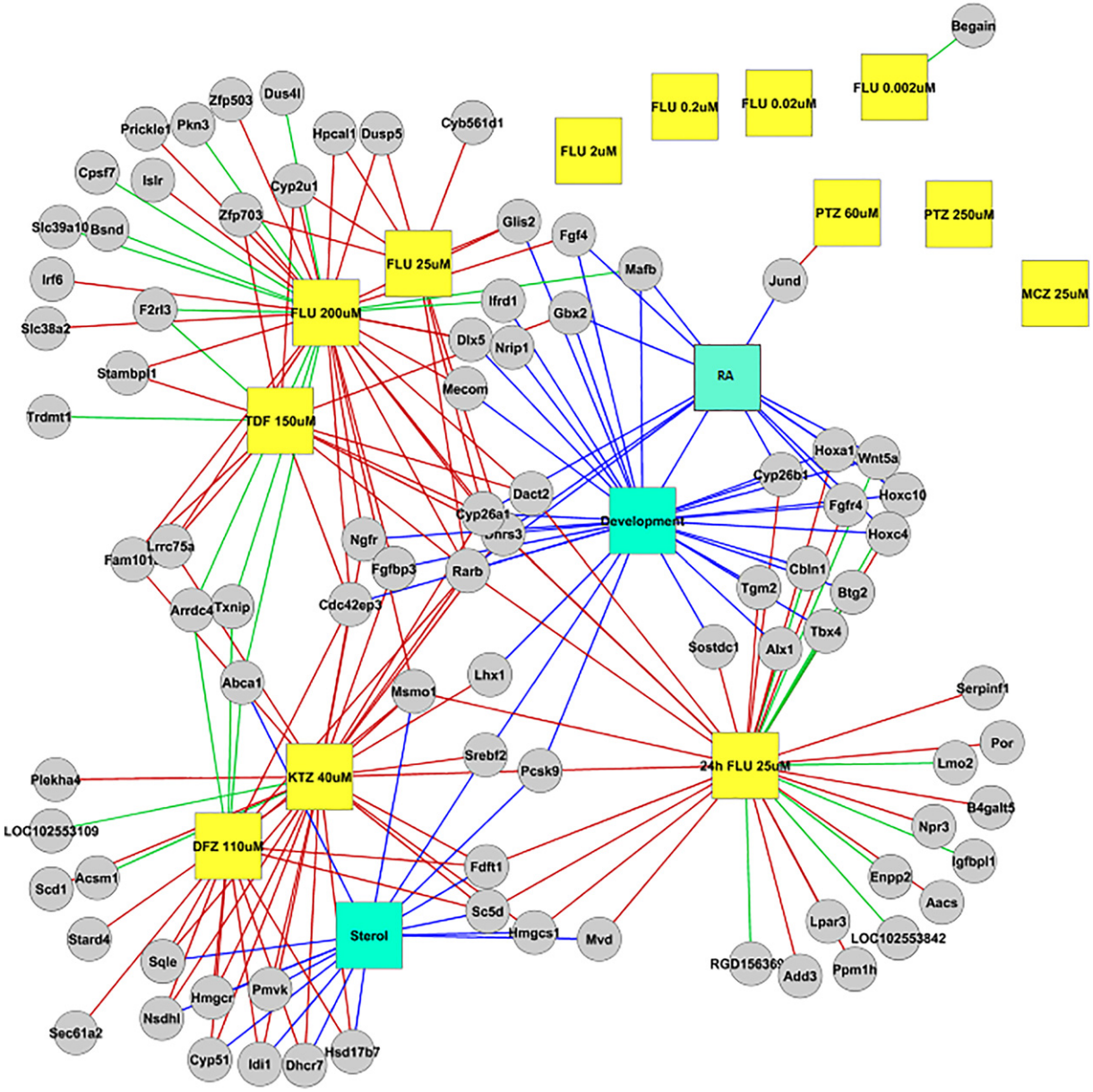

Fig. 4. Cytoscape network visualization of 87 significantly regulated genes due to rat WEC exposure to azoles. Grey cycled nodes represent the 87 genes, yellow and green squared nodes illustrate the compounds and the associated biological processes, respectively. Connections between exposure and regulated pathways demonstrate upregulation (red line), or downregulation (green line) and links of genes to pathways (blue line).

response magnitude on general embryonic development related genes (Fig. 6, B). The remaining compounds followed in the order of KTZ > MCZ ≈ DFZ > PTZ (1.21, 1.13, 1.14 and 1.09, respectively). The difference in response magnitude of this gene group between compounds was small, indicating that it mimics the morphological ID_{10} rather well. (Fig. 6, B). Interestingly, *Tbx4* was most down regulated due to WEC exposure to either MCZ or PTZ. The most upregulated genes were the aforementioned RA-related genes, as well as *Lhx1*, *Hoxa1*, *Ngfr* and *Fgfbp3*.

In contrast to the above pathways, WEC exposure to DFZ (1.423) and KTZ (1.420) appeared to have a greater effect than FLU on the sterol biosynthesis pathway. TDF had an intermediate potency, and the least potent compounds were MCZ (1.10), FLU (1.07) and PTZ (1.07). (Fig. 6, C; DFZ > KTZ > TDF > MCZ ≈ FLU ≈ PTZ). Both DFZ and KTZ upregulated *Msmo1*, *Hsd17b7* and *Sqle*. *Cyp51* was also upregulated by these two compounds, as well as by TDF. The commonly downregulated gene among the tested compounds was *Abca1*.

3.6. A comparison of gene expression responses within selected pathways between 4- and 24-h of exposure to FLU

Gene expression changes in response to FLU exposure in the RA and general embryonic development pathways varied in magnitude with exposure time. This was evident in the expression of *Cyp26a1*, *Cyp26b1*, *Hoxc10*, *Mafb* and *Wnt5a*, biomarkers of the RA pathway, (Fig. 7, A). Similarly, genes in the general embryonic development pathway showed a varied response magnitude among genes, dependent on exposure duration. In the embryonic development pathway, *Ngfr* and *Lhx1* were upregulated in embryos exposed for 4 h to almost twice the extent observed upon 24 h of exposure. In contrast, *Pcsk9* and *Tbx4* were 2-fold more responsive after the prolonged exposure than after the short exposure (Fig. 7, B).

In contrast, in the sterol biosynthesis pathway (Fig. 7, C), the magnitude of gene expression of all genes was considerably higher in embryos exposed to FLU for 24 h than in those exposed for 4 h. The sterol-related genes, *Hmgcr* and *Mvd*, only showed regulation in embryos after prolonged (24-hour) FLU-treatment.

3.7. Comparison of in vitro with in vivo data

Data on the developmental toxic profile of the six tested azoles were obtained from literature *in vivo* studies. A potency raking was performed after calculating the BMD_{10} values, evaluating incidences of skeletal malformations and cleft palate. Table 4 contains an overview of the *in vivo* calculated BMD_{10} values and dLEL values, as well as *in vitro* results from the present study, including the ID_{10} values of morphological data (TMS) and response of genes participating in the RA pathway. It should be noted that for some compounds, *e.g.* miconazole, there is a limited availability of *in vivo* data. Additional data regarding the inhibition of *Cyp26a1* are included, which were kindly provided by BASF SE laboratories of Experimental Toxicology and Ecology.

In vivo exposure to FLU, KTZ and TDF caused cleft palate, while FLU was also inducing renal malformations, such as absence of renal papilla, a type of malformation generally not typical for azoles. Furthermore, rat *in vivo* exposure to DFZ and PTZ was associated with skeletal alterations, which included formation of supernumerary rudimentary ribs, extra ossification and deformation of thoracic vertebrae. FLU and KTZ were the most potent embryotoxicants *in vivo*, following TDF and MCZ. DFZ and PTZ were the compounds with less severe effects. Data derived from the EPA *ToxRef* database were in agreement with the aforementioned observations. *In vitro* studies on the inhibition of *Cyp26a1*, after exposure to the four out of six tested compounds, show that MCZ and TDF were the most potent compounds, while PTZ and KTZ inhibited the regulation of *Cyp26a1* at higher concentrations.

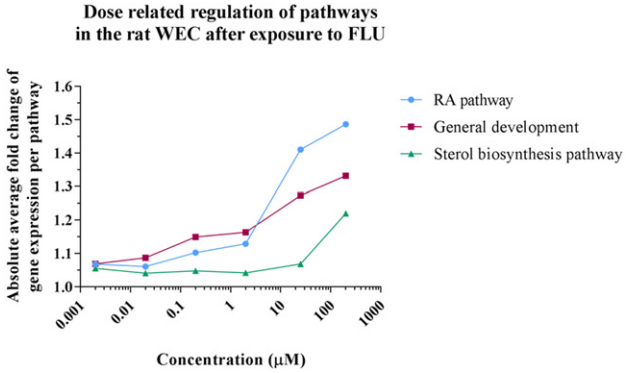

Fig. 5. Concentration-dependent effects on enriched biological processes of FLU in rat WEC, relative to the vehicle control (= 1.0), expressed as an average absolute fold change of all genes in each pathway.

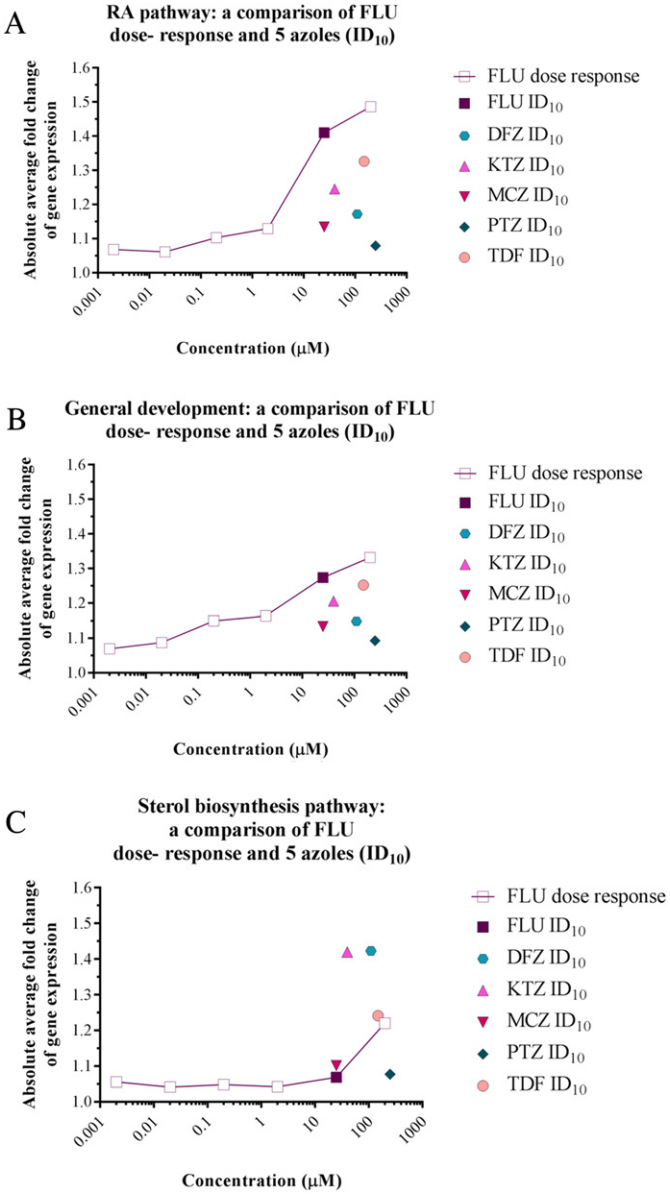

Fig. 6. Functional analysis of dose-dependent (ID_{10}) effects of tested azoles in rat WEC compared to the effects of FLU in a dose range per pathway. The response of the pathway is expressed as average fold change associated with RA pathway (A), general development (B) and sterol biosynthesis pathway (C) is compared to vehicle control (= 1.0).

4. Discussion

In agreement with previous studies (de Jong et al., 2011; Luijten et al., 2010; Robinson et al., 2012d; Menegola et al., 2005), we observed a variety of concentration dependent embryotoxic responses in rat embryos, cultured and exposed *in vitro* to six azoles for 48 h during GD 10–12. During this particular time window, major aspects of organogenesis and neurulation take place (Robinson et al., 2012a; Luijten et al., 2010; Dimopoulou et al., 2016; Mitiku and Baker, 2007). Commonly observed malformations in *in vitro* systems exposed to embryotoxic azoles were axial defects, craniofacial malformations and impaired branchial arches formation (Menegola et al., 2006a; Giavini and Menegola, 2010; Tiboni et al., 2008). KTZ and MCZ have been described to specifically affect heart function *via* dysregulating the K^+ and Ca^{2+} channels leading to heart-related syndromes (Sung et al., 2012).

In vivo developmental toxicity studies have been performed assessing the embryotoxic profile of the six tested compounds. As to cleft palate and skeletal malformations observed at gestation day 21 (GD21), FLU, KTZ and TDF were the most potent embryotoxic compounds, while MCZ, DFZ were less potent. PTZ induced embryotoxicity only at very high concentration, which are likely to be unattainable in *in vivo* situation, and thus in line with the very low embryotoxicity potential of this compound (Table 4). WEC morphology (Fig. 1, Tables 1, 2 & 4) assessed at GD12 indicated FLU, KTZ and MCZ as the most potent compounds, while TDF, DFZ and PTZ were less potent.

Following whole genome analysis in WEC exposed to each of the six azoles at their ID_{10} for effects on the TMS, we identified 87 genes significantly regulated by at least one of the tested compounds (ANOVA, $p < 0.001$). Three gene sets (DAVID) were overrepresented among the regulated genes, related to the RA pathway, general embryonic development and the sterol biosynthesis pathway, respectively (Robinson et al., 2012c; Robinson et al., 2012d). Each of the gene sets showed some regulation for all compounds tested, likely reflecting non-toxic adaptive regulation at lower concentrations, given the absence of concomitant toxic effects (Fig. 5). Such gene expression responses have been observed regularly in other systems as well (Hermsen et al., 2012; Schulpen et al., 2014). Above a certain exposure level the magnitude of regulation increased, in parallel with observed morphological effects, indicating that a threshold of adversity had been crossed (Piersma et al., 2011).

We have additionally identified genes that were significantly regulated but they did not participate in the aforementioned pathways of interest. The genes with the highest fold change were *Zfp703*, *Txnip*, *Stambpl1*, *Lrrc75a*, *Cyp2u1* and *Fam101a*, which were regulated by at least one of the tested compounds. *Zfp703*, *Lrrc75a*, *Cyp2u1* and *Fam101a* do indirectly interact with RA in rat embryos. Their significant regulation identified in embryos exposed to FLU, KTZ and TDF. They have a crucial role in repressing transcription, oxidative stress or dysregulation of bone maturation related pathways. Additionally, *Txnip* is dysregulated after rat exposure to DFZ, which could be related to responses to oxidative stress and negative regulation of cell division (National Center for Biotechnology Information, 2013; Shimoyama et al., 2015). These genes are of general interest for assessing the genomic regulation after embryonic exposure to xenobiotics.

The responsive general embryonic development gene set is involved in a variety of developmental processes and is highly dominated by RA related genes. The RA pathway has the crucial role of regulating the spatiotemporal balance of RA in the developing embryo, supporting normal growth and differentiation. Perturbations in the RA pathway may therefore be indicative of possible embryotoxicity, as they have been implicated in the toxicological mode of action of azoles (Luijten et al., 2010).

The sterol biosynthesis pathway represents the pharmacological mode of action of azoles in mammalian species. Azoles have been designed to intervene with *Cyp51*, disturbing the conversion of lanosterol to ergosterol, which stabilizes the fungal cell wall. The interference with *Cyp51* and other sterol-related genes after treatment with azole compounds, indicate their efficacy concerning the pharmacological, crop protection purposes of their application. Thus, while the RA pathway is relevant for embryotoxicity, the sterol pathway is relevant for the intended mode of action of azoles.

The 4-hour concentration-response of FLU revealed a similar curve for TMS as for the RA pathway, whereas the sterol biosynthesis pathway showed strong responses at higher exposures only, corroborating that modulation of the RA pathway, and not of the sterol biosynthesis pathway, is primarily involved in the embryotoxic response.

Furthermore, at sub-embryotoxic concentrations, FLU exposure caused an upregulation of *Tbx4* followed by a downregulation with increasing concentration, whereas *Hoxa1* showed the opposite expression pattern. Also MCZ at its ID_{10} of 25 μM showed upregulation of *Tbx4* and downregulation of both *Hoxa1* and *Hoxc4*, similarly to the gene expression profile of embryos exposed to FLU at sub-embryotoxic concentration of 0.2 μM, indicating potency differences between both compounds. *Tbx4* is regulated by *Hox* and *Wnt* gene families (Barham et al., 2009; Diez del Corral et al., 2003), the expression of which is affected by local RA levels, which would explain the effect of FLU exposure on the regulation of *Tbx4*. The observed biphasic response is intriguing. One might speculate that *Tbx4* upregulation is countered by increasing toxic responses represented by extensive regulation of the RA pathway at higher concentrations. Both *Hoxa1* and *Tbx4* have a crucial role in embryonic development, with specific sites of action at the anterior-posterior patterning and limb formation, respectively (Naiche et al., 2011; Mallo and Alonso, 2013). *Tbx4* is also as a transcription factor in the early lung mesoderm, promoting the co-ordination of *Fgf* (mainly *Fgf8*) and *Gli* proteins for the forthcoming lung development (Sakiyama et al., 2003). In the case of MCZ, the increased regulation of *Tbx4* at the ID_{10} could be also associated with the already described morphological effects on heart formation (Naiche and Papaioannou, 2003). Their non-monotonic regulation patterns with increasing exposure makes genes such as *Tbx4* and *Hoxa1* less useful as biomarkers of embryotoxic response.

As illustrated in Fig. 6 (A, B, C), rat WEC exposure to FLU, TDF and KTZ at their ID_{10} revealed marked upregulation of genes related to general embryonic development and the RA pathway, showing most extensive upregulation of *Cyp26a1* and *Dhrs3* (Fig. 3). The relative magnitude of the RA pathway regulation by the tested compounds is in line with their *in vivo* potency ranking (Table 4). Single genes within the RA pathway such as *Cyp26a1*, did not show this ranking (Table 4), indicating that whole pathway regulation may be a better indicator for embryotoxic potency than single genes (Tonk et al., 2015).

Sterol-related gene expression regulation was most extensive in embryos exposed to DFZ and KTZ (Fig. 6C). We observed the significant induction of *Cyp51*, *Msmo1*, *Hmgcr* and *Sqle*, which are indicators of increased pharmacological activity. *Cyp51* is the major biomarker of the pharmacological mode of action of our tested compounds. Among all, *Msmo1* was the highest regulated single gene. *Msmo1* role has been recently described as a determinant gene in fatty acid transcription, *via* interacting with the mammalian liver X receptors (LXRs). The LXRs are involved in the regulation of lipid and fatty acid metabolism and have an important role in central nervous system (CNS) development and, especially, in midbrain neurogenesis (Pinto et al., 2016). Additionally, LXR proteins could bind to retinoid X receptors (RXR), form heterodimers and control the regulation of gene expression. Interestingly, Gad et al. (2012) have suggested that RA and lipid metabolism related-genes, such as *Msmo1*, *Cyp51*, and *Hsd17b*, might be indirectly associated, when they tested in bovine culture both under *in vivo* and *in vitro* experimental conditions.

The occurrence and type of malformations is dependent on the timing of exposure in pregnancy (Piersma et al., 2011). The same holds for gene expression regulation by chemical exposures (Balmer et al., 2014; Luijten et al., 2010). The embryo development

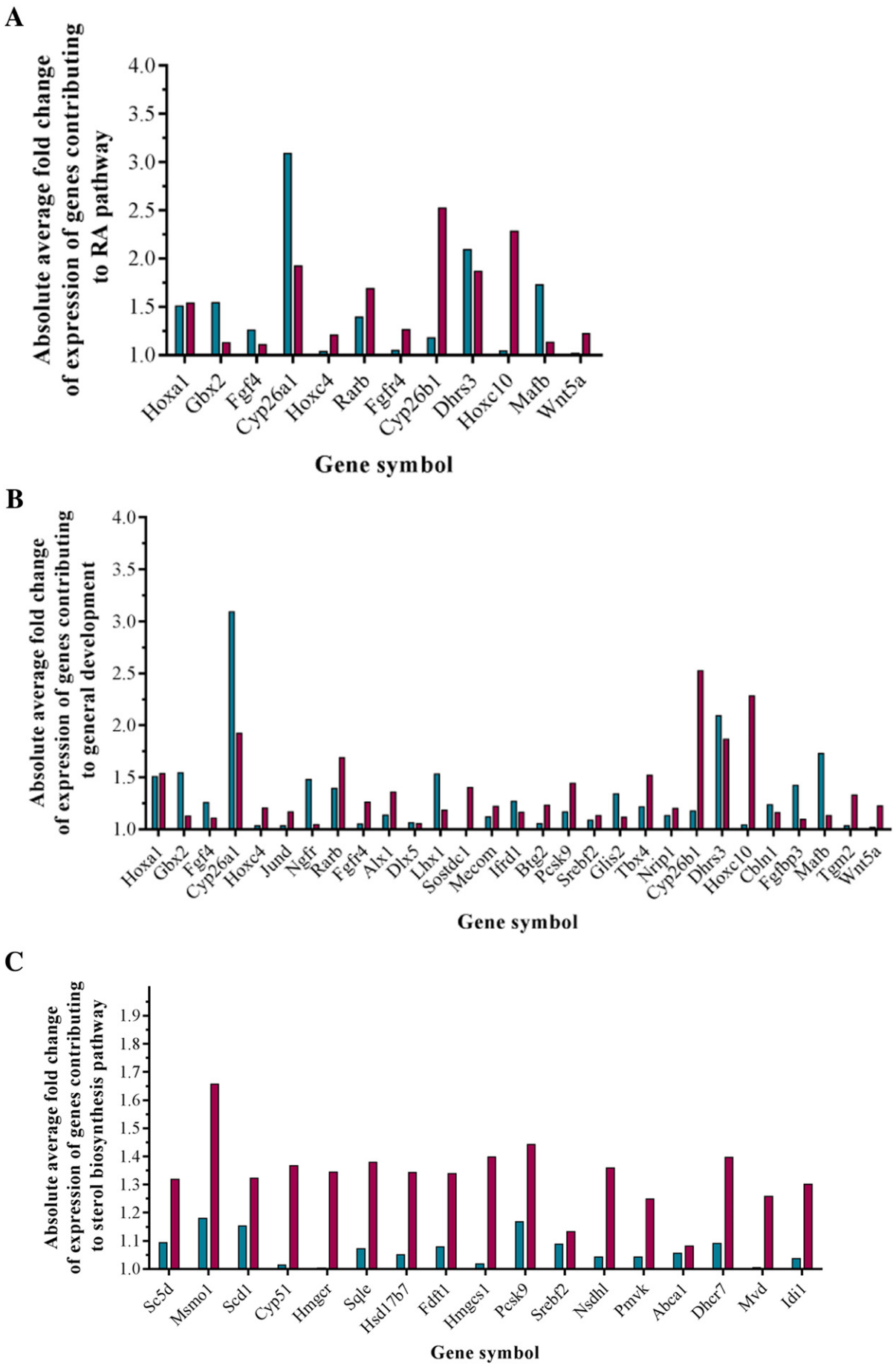
A
Absolute average fold change of expression of genes contributing to RA pathway
4.0
3.5
3.0
2.5
2.0
1.5
1.0
Hoxa1
Gbx2
Fgf4
Cyp26a1
Hoxc4
Rarb
Fgfr4
Cyp26b1
Dhrs3
Hoxc10
Mafb
Wnt5a
Gene symbol
B
Absolute average fold change of expression of genes contributing to general development
4.0
3.5
3.0
2.5
2.0
1.5
1.0
Hoxa1
Gbx2
Fgf4
Cyp26a1
Hoxc4
Jund
Ngfr
Rarb
Fgfr4
Alx1
Dlx5
Lhx1
Sostdc1
Mecom
Ifrd1
Btg2
Pcsk9
Srebf2
Glis2
Tbx4
Nrip1
Cyp26b1
Dhrs3
Hoxc10
Cbln1
Fgfbp3
Mafb
Tgm2
Wnt5a
Gene symbol
C
Absolute average fold change of expression of genes contributing to sterol biosynthesis pathway
1.9
1.8
1.7
1.6
1.5
1.4
1.3
1.2
1.1
1.0
Sc5d
Msmo1
Scd1
Cyp51
Hmgcr
Sqle
Hsd17b7
Fdft1
Hmgcs1
Pcsk9
Srebf2
Nsdhl
Pmvk
Abca1
Dhcr7
Mvd
Idi1
Gene symbol

Table 4
Overview of *in vivo* and *in vitro* developmental toxicity data of the tested azoles.

Compound	*In vivo*		*In vitro*		
	BMD_{10} (μmol/kg)	dLEL (μmol/kg) (USEPA, 2016)	ID_{10} (TMS)	RA response (abs fold change)	IC_{50} *Cyp26a1* inhibition (μM)
PTZ	917.8 (Stahl, 1997)	290.8	250	1.08	3.02
DFZ	596.5 (Lochry, 1987)	421.5	110	1.17	–
MCZ	258.3 (Ito et al., 1976)	–	25	1.13	0.44
TDF	91.5 (Machemer, 1976; Unger et al., 1982)	171.4	150	1.33	2.29
KTZ	20.1 (Nishikawa et al., 1984; Tachibana et al., 1987)	–	40	1.25	12.02
FLU	9.1 (Lamontia et al., 1984)	1.3	25	1.41	–

gene set showed time-dependent higher as well as lower regulation of individual genes, whereas the sterol pathway consistently showed higher gene expression responses after longer exposure. In the sterol pathway, *Msmo1*, *Cyp51*, *Hmgr*, *Sqle* and *Pcsk9* were the most quantitatively pronounced genes at 24 h-FLU exposed embryos, which are involved in the cascade of sterol related enzymatic reactions (Larsen et al., 2011).

Furthermore, among the RA-related genes *Cyp26a1*, *Dhrs3*, *Mafb* and *Gbx2* were more upregulated in 4 h than 24 h FLU exposed embryos (MacLean et al., 2001). *Cyp26a1*, *Dhrs3* and *Mafb* play a role in determining RA levels in the embryo. On the other hand, *Cyp26b1* and *Hoxc10* were relatively highly upregulated at the later time point. These genes have a different expression pattern in the embryo as compared to *e.g. Cyp26a1*. Additionally, there was a higher regulation of *Ngfr*, *Lhx1* and *Fgfbp3* in 4-hour exposed embryos to FLU, compared to 24-hour of exposure. These genes are important contributors to general embryonic development. *Ngfr* has a crucial role in the development of neurons in the embryonic brain, while it has been suggested as a mediator for activating thyroid hormone (Porterfield, 2000). *Lhx1* has been suggested to co-operate with *Pax6* in mouse embryos for forming the anterior thalamus (Hevner et al., 2002; Pratt et al., 2000). Another study about the development of *Xenopus* and chick embryos has shown that *Lhx1* is a transcription factor for nephric duct formation during development, which is triggered by RA and is collaborating with *Hox* genes, *Pax2* and *Pax8* transcriptional factors for further activation of *Gata3* and the *Wnt* signalling pathway (Costantini and Kopan, 2010). These observations illustrate the spatiotemporal differences in sensitivity of regulatory processes in embryogenesis, the perturbation of which underlies the specification of malformations. This aspect is likewise important when employing gene expression data for toxicity profiling.

Comparing the RA-with the sterol biosynthesis pathway, our data indicate that those compounds which more strongly affect the RA pathway, belong to the group of embryotoxic ones, whereas those who affect the sterol biosynthesis pathway, or those who have low activity on both pathways are less embryotoxic.

The data also show other differences in gene expression pattern that could be used to elucidate additional pathways involved in embryotoxicity. This analysis shows the usefulness of investigation of gene expression modulation to obtain mechanistic information pertinent to assess the toxicity *versus* functional efficacy of chemicals. The comparison of relatively simple markers such as *Cyp26a1* for the RA pathway (undesired or off target effects) and *Cyp51* for the sterol biosynthesis pathway (pharmacological or on-target effect) could potentially be used for the optimization in the development of new compounds.

Conflict of interest

The authors declare that there are no conflicts of interest.

Transparency document

The Transparency document associated with this article can be found, in online version.

Acknowledgement

This work was supported by a collaborative project between Wageningen University, RIVM, and BASF SE.

References

Augustine-Rauch, K., Zhang, C.X., Panzica-Kelly, J.M., 2010. In vitro developmental toxicology assays: a review of the state of the science of rodent and zebrafish whole embryo culture and embryonic stem cell assays. Birth Defects Res. C Embryo Today 90 (2), 87–98.

Balmer, N.V., et al., 2014. From transient transcriptome responses to disturbed neurodevelopment: role of histone acetylation and methylation as epigenetic switch between reversible and irreversible drug effects. Arch. Toxicol. 88 (7), 1451–1468.

Barham, G., Clarke, Nicholas, M.P., 2009. Genetic regulation of embryological limb development with relation to congenital limb deformity in humans. J. Child. Orthop. 2 (1), 1–9.

Brown, N.A., Fabro, S., 1981. Quantitation of rat embryonic development in vitro: a morphological scoring system. Teratology 24 (1), 65–78.

Costantini, F., Kopan, R., 2010. Patterning a complex organ: branching morphogenesis and nephron segmentation in kidney development. Dev. Cell 18 (5), 698–712.

Cunningham, T.J., Duester, G., 2015. Mechanisms of retinoic acid signalling and its roles in organ and limb development. Nat. Rev. Mol. Cell Biol. 16 (2), 110–123.

Dai, M., et al., 2005. Evolving gene/transcript definitions significantly alter the interpretation of GeneChip data. Nucleic Acids Res. 33 (20), e175.

Daston, G.P., Naciff, J.M., 2010. Predicting developmental toxicity through toxicogenomics. Birth Defects Res. C Embryo Today 90 (2), 110–117.

Diez del Corral, R., et al., 2003. Opposing FGF and retinoid pathways control ventral neural pattern, neuronal differentiation, and segmentation during body axis extension. Neuron 40 (1), 65–79.

Dimopoulou, M., Verhoef, A., van Ravenzwaay, B., Rietjens, I.M., Piersma, A.H., 2016. Flusilazole induces spatio-temporal expression patterns of retinoic acid-, differentiation- and sterol biosynthesis-related genes in the rat Whole Embryo Culture. Reprod. Toxicol. 64, 77–85.

Eijssen, L.M., et al., 2013. User-friendly solutions for microarray quality control and preprocessing on ArrayAnalysis.org. Nucleic Acids Res. 41, W71–W76 (Web Server issue).

Ellis-Hutchings, R.G., Carney, E.W., 2010. Whole embryo culture: a "new" technique that enabled decades of mechanistic discoveries. Birth Defects Res. B Dev. Reprod. Toxicol. 89 (4), 304–312.

Farag, A.T., Ibrahim, H.H., 2007. Developmental toxic effects of antifungal flusilazole administered by gavage to mice. Birth Defects Res. B Dev. Reprod. Toxicol. 80 (1), 12–17.

Flick, B., et al., 2009. Embryotoxic potential of *N*-methyl-pyrrolidone (NMP) and three of its metabolites using the rat whole embryo culture system. Toxicol. Appl. Pharmacol. 237 (2), 154–167.

Gad, A., et al., 2012. Molecular mechanisms and pathways involved in bovine embryonic genome activation and their regulation by alternative in vivo and in vitro culture conditions. Biol. Reprod. 87 (4), 100.

Genschow, E., et al., 2002. The ECVAM international validation study on in vitro embryotoxicity tests: results of the definitive phase and evaluation of prediction models. European Centre for the VALIDATION of Alternative Methods. Altern. Lab. Anim 30 (2), 151–176.

Giavini, E., Menegola, E., 2010. Are azole fungicides a teratogenic risk for human conceptus? Toxicol. Lett. 198 (2), 106–111.

Fig. 7. A comparison of gene expression regulation in embryos exposed for 4 (blue) or 24 h (red) to FLU at 25 μM (ID_{10}) per functional pathway, RA pathway (A), general development (B) and sterol biosynthesis pathway (C).

Hermsen, S.A., et al., 2011. Relative embryotoxicity of two classes of chemicals in a modified zebrafish embryotoxicity test and comparison with their in vivo potencies. Toxicol. in Vitro 25 (3), 745–753.
Hermsen, S.A., et al., 2012. Triazole-induced gene expression changes in the zebrafish embryo. Reprod. Toxicol. 34 (2), 216–224.
Hevner, R.F., Miyashita-Lin, E., Rubenstein, J.L., 2002. Cortical and thalamic axon pathfinding defects in Tbr1, Gbx2, and Pax6 mutant mice: evidence that cortical and thalamic axons interact and guide each other. J. Comp. Neurol. 447 (1), 8–17.
Huang da, W., Sherman, B.T., Lempicki, R.A., 2009. Systematic and integrative analysis of large gene lists using DAVID bioinformatics resources. Nat. Protoc. 4 (1), 44–57.
Irizarry, R.A., et al., 2003. Exploration, normalization, and summaries of high density oligonucleotide array probe level data. Biostatistics 4 (2), 249–264.
Ito, C., Shibutanil, Y., Inoue, K., Nakano, K., Ohnishi, H., 1976. Toxicologocal studies of miconazole (II) teratological studies of miconazole in rats. Iyakuhin Kenkyu 7 (3), 367–376.
van der Jagt, K.M.S., Tørsløv, J., de Bruijn, J., 2004. Alternative approaches can reduce the use of test animals under Reach European Commission Directorate General Jrc Joint Research Centre Institute for Health and Consumer Protection. http://home.kpn.nl/reach/downloads/reducingtheuseoftestanimalsunderreachihcprepor.pdf.
de Jong, E., et al., 2011. Comparison of the mouse embryonic stem cell test, the rat whole embryo culture and the zebrafish embryotoxicity test as alternative methods for developmental toxicity testing of six 1,2,4-triazoles. Toxicol. Appl. Pharmacol. 253 (2), 103–111.
Lamontia, C.L., S.R., Alvarez, L., 1984. Embryo-fetal Toxicity and Teratogenicity Study of INH-6573-39 by Gavage in the Rat. Unpublished Reports No. HLR 444-83 and HLR 142-84 From Haskell Laboratory for Toxicology and Industrial Medicine, Wilmington, Delaware, USA. Submitted to WHO by E.I. du Pont de Nemours & Co., Inc., Wilmington, Delaware, USA. Summarized in JMPR Monograph—Flusilazole, Pesticide Residues in Food: 1995 Evaluations Part II Toxicological & EnvironmentEnvironment. (http://www.inchem.org/documents/jmpr/jmpmono/v95pr08.htm).
Larsen, L., et al., 2011. Expression and localization of microRNAs in perinatal rat pancreas: role of miR-21 in regulation of cholesterol metabolism. PLoS One 6 (10), e25997.
Lee, H.Y., et al., 2012. Alternative models in developmental toxicology. Syst. Biol. Reprod. Med. 58 (1), 10–22.
Li, Z., et al., 2012. Vitamin A deficiency induces congenital spinal deformities in rats. PLoS One 7 (10), e46565.
Lochry, E.A., 1987. Developmental Toxicity Study of CGA-169374 technical (FL-851406) Administreted Orally Via Gavage to Crl:COBS CD (SD) BR Presumed Pregnant Rats. Unpublished report No. 203-005 From Novartis Crop Protection AG., Basel, Switzerland and Argus Research Lab. Inc., Horsham, USA, Submitted to WHO by SYgenta Crop Protection AG, Basel, Switzerland. (http://apps.who.int/iris/bitstream/10665/44064/1/9789241665230_eng.pdf?ua=1).
Luijten, M., et al., 2008. Application of a metabolizing system as an adjunct to the rat whole embryo culture. Toxicol. in Vitro 22 (5), 1332–1336.
Luijten, M., et al., 2010. Transcriptomics analysis of retinoic acid embryotoxicity in rat postimplantation whole embryo culture. Reprod. Toxicol. 30 (2), 333–340.
Machemer, L., 1976. Evaluation of Embryotoxic and Teratogenic Effects on Rats Following Oral Administration. Report no. 6294, Bayer AG, Institut für Toxikologie, submitted by Bayer AG to WHO. ((Unpublished), http://www.inchem.org/documents/jmpr/jmpmono/v81pr32.htm).
MacLean, G., et al., 2001. Cloning of a novel retinoic-acid metabolizing cytochrome P450, Cyp26B1, and comparative expression analysis with Cyp26A1 during early murine development. Mech. Dev. 107 (1–2), 195–201.
Mallo, M., Alonso, C.R., 2013. The regulation of Hox gene expression during animal development. Development 140 (19), 3951–3963.
Marotta, F., Tiboni, G.M., 2010. Molecular aspects of azoles-induced teratogenesis. Expert Opin. Drug Metab. Toxicol. 6 (4), 461–482.
McCaffery, P.J., et al., 2003. Too much of a good thing: retinoic acid as an endogenous regulator of neural differentiation and exogenous teratogen. Eur. J. Neurosci. 18 (3), 457–472.
Menegola, E., et al., 2005. Craniofacial and axial skeletal defects induced by the fungicide triadimefon in the mouse. Birth Defects Res. B Dev. Reprod. Toxicol. 74 (2), 185–195.
Menegola, E., et al., 2006a. Dysmorphogenic effects of some fungicides derived from the imidazole on rat embryos cultured in vitro. Reprod. Toxicol. 21 (1), 74–82.
Menegola, E., et al., 2006b. Postulated pathogenic pathway in triazole fungicide induced dysmorphogenic effects. Reprod. Toxicol. 22 (2), 186–195.
Mitiku, N., Baker, J.C., 2007. Genomic analysis of gastrulation and organogenesis in the mouse. Dev. Cell 13 (6), 897–907.
Naiche, L.A., Papaioannou, V.E., 2003. Loss of Tbx4 blocks hindlimb development and affects vascularization and fusion of the allantois. Development 130 (12), 2681–2693.
Naiche, L.A., et al., 2011. Identity and fate of Tbx4-expressing cells reveal developmental cell fate decisions in the allantois, limb, and external genitalia. Dev. Dyn. 240 (10), 2290–2300.
Database resources of the National Center for Biotechnology Information. Nucleic Acids Res., 2013. 41(Database issue): p. D8–d20.
New, D.A., Coppola, P.T., Cockroft, D.L., 1976. Comparison of growth in vitro and in vivo of post-implantation rat embryos. J. Embryol. Exp. Morpholog. 36 (1), 133–144.
Nishikawa, S., H.T., Muyazaki, H., Ohguro, Y., 1984. Reproduction studies of KW-144 in rats and rabbits. Kiso To Rinsho (Clin. Rep.) 18, 1433–1448.
Piersma, A.H., 1993. Whole embryo culture and toxicity testing. Toxicol. in Vitro 7 (6), 763–768.
Piersma, A.H., 2004. Validation of alternative methods for developmental toxicity testing. Toxicol. Lett. 149 (1–3), 147–153.
Piersma, A.H., 2006. Alternative methods for developmental toxicity testing. Basic Clin. Pharmacol. Toxicol. 98 (5), 427–431.
Piersma, A.H., et al., 1995. Interlaboratory evaluation of embryotoxicity in the postimplantation rat embryo culture. Reprod. Toxicol. 9 (3), 275–280.
Piersma, A.H., et al., 2011. Reproductive toxicants have a threshold of adversity. Crit. Rev. Toxicol. 41 (6), 545–554.
Pinto, C.L., et al., 2016. Lxr regulates lipid metabolic and visual perception pathways during zebrafish development. Mol. Cell. Endocrinol. 419, 29–43.
Porterfield, S.P., 2000. Thyroidal dysfunction and environmental chemicals: potential impact on brain development. Environ. Health Perspect. 108, 433–438.
Pratt, T., et al., 2000. A role for Pax6 in the normal development of dorsal thalamus and its cortical connections. Development 127 (23), 5167–5178.
Robinson, J.F., et al., 2010. Embryotoxicant-specific transcriptomic responses in rat postimplantation whole-embryo culture. Toxicol. Sci. 118 (2), 675–685.
Robinson, J.F., Verhoef, A., Piersma, A.H., 2012a. Transcriptomic analysis of neurulation and early organogenesis in rat embryos: an in vivo and ex vivo comparison. Toxicol. Sci. 126 (1), 255–266.
Robinson, J.F., Pennings, J.L., Piersma, A.H., 2012b. A review of toxicogenomic approaches in developmental toxicology. Methods Mol. Biol. 889, 347–371.
Robinson, J.F., et al., 2012c. A comparison of gene expression responses in rat whole embryo culture and in vivo: time-dependent retinoic acid-induced teratogenic response. Toxicol. Sci. 126 (1), 242–254.
Robinson, J.F., et al., 2012d. Triazole induced concentration-related gene signatures in rat whole embryo culture. Reprod. Toxicol. 34 (2), 275–283.
Robinson, J.F., Gormley, M.J., Fisher, S.J., 2016. A genomics-based framework for identifying biomarkers of human neurodevelopmental toxicity. Reprod. Toxicol. 60, 1–10.
Sakiyama, J., Yamagishi, A., Kuroiwa, A., 2003. Tbx4-Fgf10 system controls lung bud formation during chicken embryonic development. Development 130 (7), 1225–1234.
Schulpen, S.H., et al., 2014. A statistical approach towards the derivation of predictive gene sets for potency ranking of chemicals in the mouse embryonic stem cell test. Toxicol. Lett. 225 (3), 342–349.
Scialli, A.R., 2008. The challenge of reproductive and developmental toxicology under REACH. Regul. Toxicol. Pharmacol. 51 (2), 244–250.
Scialli, A.R., Guikema, A.J., 2012. REACH and reproductive and developmental toxicology: still questions. Syst. Biol. Reprod. Med. 58 (1), 63–69.
Shimoyama, M., et al., 2015. The rat genome database 2015: genomic, phenotypic and environmental variations and disease. Nucleic Acids Res. 43, D743–D750 (Database issue).
Slob, W., 2002. Dose-response modeling of continuous endpoints. Toxicol. Sci. 66 (2), 298–312.
Smoot, M.E., et al., 2011. Cytoscape 2.8: new features for data integration and network visualization. Bioinformatics 27 (3), 431–432.
Sogorb, M.A., et al., 2014. An integrated approach for detecting embryotoxicity and developmental toxicity of environmental contaminants using in vitro alternative methods. Toxicol. Lett. 230 (2), 356–367.
Spielmann, H., 2009. The way forward in reproductive/developmental toxicity testing. Altern. Lab. Anim 37 (6), 641–656.
Stahl, B., 1997. JAU 6476 - Developmental Toxicity Study in Rats After Oral Administration. Unpublished Report No. M-012279-01-1 from Bayer AG, Wuppertal, Germany. Submitted to WHO by Bayer CropScience AG, Germany. (https://www.google.nl/url?sa=t&rct=j&q=&esrc=s&source=web&cd=2&ved=0ahUKEwjcjNCx5-HPAhWDrxoKHebSDzYQFgghMAE&url=http%3A%2F%2Fapps.who.int%2Fpesticide-residues-jmpr-database%2FDocument%2F110&usg=AFQjCNGpjQOE2xfb0QbWPWwA5-avbrC8kQ&sig2=ZFM7G3fgK4EdIA0e_zX0hQ&cad=rja).
Sung, D.J., et al., 2012. Blockade of K+ and Ca2+ channels by azole antifungal agents in neonatal rat ventricular myocytes. Biol. Pharm. Bull. 35 (9), 1469–1475.
Tachibana, M.N., Y, Monro, A.M., 1987. Toxicology of fluconazole in experimental animals. In: Fromtling, R.A. (Ed.), Recent Trends in the Discovery, Development, and Evaluation of Antifungal Agents. JR Prous, Barcelona, pp. 93–102.
Tiboni, G.M., Marotta, F., Castigliego, A.P., 2008. Teratogenic effects in mouse fetuses subjected to the concurrent in utero exposure to miconazole and metronidazole. Reprod. Toxicol. 26 (3–4), 254–261.
Tonk, E.C., Pennings, J.L., Piersma, A.H., 2015. An adverse outcome pathway framework for neural tube and axial defects mediated by modulation of retinoic acid homeostasis. Reprod. Toxicol. 55, 104–113.
Unger, T.M., Van Goethem, D., Shellenberger, 1982. A Teratological Evaluation of Bayleton in Mated Female Rats. Midwest Research Institute, Report No. 324 to Mobay Chemical Corporation Agricultural Chemical Division submitted to WHO by Bayer AG. ((Unpublished), http://www.inchem.org/documents/jmpr/jmpmono/v83pr39.htm).
USEPA, 2016. Animal Toxicity Studies: Effects and Endpoints (Toxicity Reference Database - ToxRefDB files). (Retrieved from ftp://newftp.epa.gov/comptox/High_Throughput_Screening_Data/Animal_Tox_Data/on June 2016).
Webster, W.S., Brown-Woodman, P.D., Ritchie, H.E., 1997. A review of the contribution of whole embryo culture to the determination of hazard and risk in teratogenicity testing. Int. J. Dev. Biol. 41 (2), 329–335.
Zarn, J.A., Bruschweiler, B.J., Schlatter, J.R., 2003. Azole fungicides affect mammalian steroidogenesis by inhibiting sterol 14 alpha-demethylase and aromatase. Environ. Health Perspect. 111 (3), 255–261.